Cyclic Resistance of High Plasticity North Java Clays and Silt

E. Rismantojo[1], E. Ginting[1], and M. Ochoa[2]
[1]*Civil Engineering Department, Institute of Technology Bandung (ITB), Bandung, Indonesia*
[2]*Tolunay-Wong Engineers Inc., 10710 South Sam Houston Pkwy West, Suite 100, Houston, TX, USA*
E-mail: erza@si.itb.ac.id

ABSTRACT: In an attempt to develop a database of the cyclic resistance of fine-grained soils in Indonesia a series of cyclic triaxial test was performed on fine-grained soils collected from two locations near shore of north Java Island, Indonesia. These samples were classified as fine-grained soils with clay-like behavior and, according to various liquefaction criteria, they are non-liquefiable. Our study used a cyclic triaxial test to apply multistage cyclic axial stresses in a form of sinusoidal stress with a frequency of 1 Hz. All specimens are isotropically consolidated passing their preconsolidation stress in order to achieve a normally consolidated state with OCR of about 1. Our findings suggest that cyclic resistance of North Java clay-like fine-grained soils follows the SHANSEP concept and could be normalized at OCR of 1. At fifteen cycles of uniform sinusoidal loading the tested clay and silt samples have a normalized cyclic strength, $(q_{cyc}/2)/\sigma_c'$, or a cyclic resistance ratio (CRR) of approximately 0.31 and a cyclic strength ratio, $(q_{cyc}/2)/s_u$, of 0.70.

KEYWORDS: Clay-like behavior, Cyclic resistance ratio, Cyclic strength ratio, Plasticity index, Water content to liquid limit ratio.

1. INTRODUCTION

Saturated fine-grained soils that behave like clays are usually considered not susceptible to liquefaction. However, under a certain earthquake condition the cyclic induced strain of saturated clays can be high enough to experience a liquefaction-like condition. Boulanger and Idriss (2004, 2006, 2007) reported a case where a ground settlement experienced by an instrumented fill embankment during 1999 Kocaeli Turkey earthquake is partly attributed to the vertical deformation of a high plasticity clay (CH) layer underneath the embankment. Their findings emphasize the important of analyzing the cyclic resistance and their associated cyclic induced strain of saturated clays in foundation design and site preparation.

Our study focuses on North Java clays and silt behavior under cyclic loading. Java is the most populated island in Indonesia. The majority of Java island consists of highlands and mountains while the rest is lowlands and coastal plains. Various major infrastructure developments such as power plants and seaports are constructed in north Java coastal area. North Java coastal alluvial plains consist generally of unconsolidated clay and sand of Quaternary age with thickness of 50 meters or more. The upper layers are usually very soft to soft and require soil improvement by vertical drainage installation with preloading or vacuum methods. The common practice in Indonesia is that clays are considered not susceptible to liquefaction and no further analysis is usually carried out to determine their safety against cyclic failure or their stability against deformation due to cyclic induced strain.

Boulanger and Idriss (2004, 2006) suggested that the behavior of fine-grained soils under cyclic load can be categorized into three groups, i.e., fine-grained soils that behave like sand, fine-grained soils that behave like clay, and fine-grained soils that behave in transition between sand and clay. Various researchers have published different liquefaction criterion to screen out fine-grained soils that behave like clay and not susceptible to liquefaction from those that behave like sand and susceptible to liquefaction. The liquefaction criterion commonly used in Indonesia is the Chinese Criterion (Wang 1981) or the Modified Chinese Criterion (Seed and Idriss 1982; Seed et al. 1983). The Modified Chinese Criterion states that clayey soils above A-line is susceptible to liquefaction if they contain less than 15% particles smaller than 0.005 mm, liquid limit (*LL*) less than 35, and ratio between natural water content and liquid limit, w_c/LL, greater than 0.90. This criterion suggests that fine-grained soils with more than 15% particle smaller than 0.005 mm with *LL* of more than 35 are not susceptible to liquefaction. Further studies by other researchers identified that *PI*, in addition to percent clay and w_c/LL, is also an important factor as liquefaction parameter of fine-grained soils. For example, Bray and Sancio (2006) suggested that clays with PI > 18 at any w_c/LL ratio are not susceptible to liquefaction except for sensitive clays that may still experience significant strength loss due to cyclic induced straining. Bol et al. (2010) proposed *LL*, liquidity index (*LI*), % clay content (particle size < 0.002 mm), and mean particle diameter (D_{50}) as parameters for liquefaction criterion and suggest that fine-grained soils with *LL* > 33 and/or % clay content > 15 are not susceptible to liquefaction. Recent study by Pathak and Purandare (2016) found that effective overburden pressure, σ_v', combined with w_c/LL, PI, D_{50}, and % clay content (< 0.002 mm) provides a criterion that gives a high success rate of predicting liquefaction for fine-grained soils compared to other available liquefaction criteria. Their finding suggests that fine-grained soils with % clay content > 15, *PI* > 25, and effective overburden > 250 kPa are not susceptible to liquefaction. According to the liquefaction criterion mentioned above the samples used in this study are categorized as not susceptible to liquefaction.

Despite being considered as not susceptible to liquefaction, clays subjected to cyclic loading may experience cyclic mobility where the accumulation of strain can yield a liquefaction-like condition. It is thus important to determine the cyclic strength of clays and their associated cyclic induced strain. Studies by Boulanger and Idriss (2004, 2006, 2007) on cyclic failure of clays found that the cyclic resistance of clays is empirically related to their normalized undrained shear strength and loading history. Based on their findings we focused our study not only on the cyclic strength of North Java clays and silts but also on the derivation of their normalized cyclic strength and relation to loading history.

1.1 Cyclic Resistance Ratio of Clay-like Behavior of Fine-Grained Soils

Boulanger and Idriss (2004, 2006, 2007) developed a relationship, based on normalized undrained shear strength, to determine the cyclic resistance ratio of clay-like behavior fine-grained soils at any earthquake magnitude CRR_M. Based on Direct Simple Shear (*DSS*) cyclic test results for soils consolidated to an effective vertical stress σ_{vc}' the relationship in its complete form, where the corrections for two-dimensional load direction, earthquake magnitude, and initial static shear stress are included, is given in Eq. (1)

$$CRR_M = \left(\frac{\tau_{cyc}}{\sigma_{vc}'}\right)_M = C_{2D} \cdot \left(\frac{\tau_{cyc}}{s_u}\right)_{M=7.5} \cdot \frac{s_u}{\sigma_{vc}'} \cdot MSF \cdot K_\alpha \quad (1)$$

Table 1 Sample Characteristics

Sample No.	Depth (m)	USCS	$< 75\mu m$[1] (%)	$< 5\mu m$[2] (%)	$< 2\mu m$[3] (%)	D_{50}[4] (mm)	Atterberg Limits			e_o	P_c' (kPa)	SPT[5]
							LL	*PL*	*PI*			
S1	15 – 16	Fat clay (CH)	92.78	63.98	42.50	0.0030	97	33	64	1.34	93.5	0/45 – 4/30 (0 – 4.3)
S2	16 – 17	Fat clay (CH)	96.84	67.50	47.40	0.0022	122	31	91	1.25	97.1	0/45 – 7/30 (0 – 7.6)
S3	17 – 18	Fat clay (CH)	96.94	79.53	67.80	-	109	35	74	1.34	197.1	0/45 – 3/30 (0 – 3.3)
S5	20 – 21	Fat clay (CH)	96.88	56.27	38.80	0.0036	94	34	60	1.70	97.1	1/45 – 3/30 (1.1 – 3.3)
S6	5 – 6	Elastic silt (MH)	88.94	23.73	56.27	0.0295	51	31	20	1.53	87.3	1/50 (0.9)

Notes: [1]Fines content with particle size of less than 0.075 mm
[2]Clay content with particle size of less than 0.005 mm
[3]Clay content with particle size of less than 0.002 mm
[4]Mean particle size
[5]Measured SPT values in blows per cm of penetration. The values in parentheses are the corrected SPT N_{60} in blows/30 cm penetration

where,

C_{2D} = correction for two-dimensional versus one-dimensional cyclic loading

$\left(\tau_{cyc}/s_u\right)_{M=7.5}$ = cyclic strength ratio (ratio of DSS one-dimensional cyclic stress to undrained shear strength s_u for the number of equivalent uniform cycles representative of a M_w=7.5 earthquake)

MSF = earthquake magnitude scale factor

K_α = correction factor for static shear stress ratio

The above equation incorporated the normalized undrained shear strength, s_u/σ'_{vc}, a concept that was introduced by Ladd and Foott (1974) and known as SHANSEP (Stress History and Normalized Engineering Properties) model. Ladd and Foott (1974) suggested that s_u/σ'_{vc} of most non-structured clays is governed by the normalized undrained shear strength at the normally-consolidated state, the stress history, as well as the soil mineralogy. The equation for the normalized undrained shear strength described above is given in Eq. (2) where *m* is a material specific coefficient.

$$\frac{s_u}{\sigma'_{vc}} = \left(\frac{s_u}{\sigma'_{vc}}\right)_{OCR=1} \times OCR^m \quad (2)$$

Based on Eqs. (1) and (2) above the *CRR* of a clay consolidated to any *OCR* value, with no applied initial static shear stress, and subjected to a *DSS* cyclic test can be defined by Eq. (3).

$$CRR = \frac{\tau_{cyc}}{\sigma'_{vc}} = \frac{\tau_{cyc}}{s_u} \times \left(\frac{s_u}{\sigma'_{vc}}\right)_{OCR=1} \times OCR^m \quad (3)$$

Boulanger and Idriss (2007) studied the results of various works of other researchers and suggested that clays having *OCR* between 1 and 4 subjected to 30 cycles of *DSS* cyclic loading have an average cyclic strength ratio τ_{cyc}/s_u of 0.83. Boulanger and Idriss (2006, 2007) also suggested that variation of clay minerals did not appear to have influence on the cyclic strength ratio and implied that this ratio may be a constant, at least, for the soils under their study. If our understanding is correct, then Eq. (3) can be further modified to Eqs. 4 and 5. If we use a variable *r* for τ_{cyc}/s_u and that this cyclic strength ratio is a constant then

$$CRR = \frac{\tau_{cyc}}{\sigma'_{vc}} = r \times \left(\frac{s_u}{\sigma'_{vc}}\right)_{OCR=1} \times OCR^m$$

$$= \left(\frac{r \times s_u}{\sigma'_{vc}}\right)_{OCR=1} \times OCR^m \quad (4)$$

$$\therefore CRR = \frac{\tau_{cyc}}{\sigma'_{vc}} = \left(\frac{\tau_{cyc}}{\sigma'_{vc}}\right)_{OCR=1} \times OCR^m \quad (5)$$

The *CRR* of clays in Eq. (5) is now expressed as normalized cyclic strength similar to the SHANSEP normalized undrained shear strength in Eq. (2). Our study used a cyclic triaxial equipment instead of *DSS*. In a cyclic triaxial test the *CRR* is defined as $\left(q_{cyc}/2\right)/\sigma'_c$ where q_{cyc} is the cyclic deviatoric axial stress and σ'_c is the effective confining consolidation stress. Our current findings suggested that cyclic strength of clay soils can be normalized, at least at *OCR* of 1, and that we need further study to determine whether the normalized cyclic strength of clay soils are influenced by the stress history in the way indicated by Eq. (5).

The relationship between *CRR* and the number uniform cyclic load is expressed by Eq. (6)

$$CRR = aN^{-b} \quad (6)$$

where N is the number of uniform stress cycles. For clays Boulanger and Idriss (2004) suggested an average b = 0.135 for DSS test and b = 0.109 for triaxial test. Therefore, if a *CRR* at certain number of uniform cyclic load is known then the *CRR* at a different number cyclic load can be estimated by Eq. (7)

$$\frac{N_A}{N_B} = \left(\frac{CRR_B}{CRR_A}\right)^{\frac{1}{b}} \quad (7)$$

Boulanger and Idriss (2004) studied 124 recorded earthquake time histories from 13 sites with earthquakes magnitudes between 7 and 8 and suggested that for clays the number of equivalent uniform cycles, at a uniform stress ratio equal to 65% of the peak stress, is about 30. Our study used a cyclic triaxial test and subjected four of the test specimens with 15 and one with 30 uniform stress cycles. Based on Eq. (7) with b = 0.109 the *CRR* at 30 load cycles should be approximately 0.927 of that at 15 load cycles.

2. RESEARCH METHOD

2.1 Sample Collection

Five soil samples were used in this research and they were collected from two near-shore locations in coastal areas of the northern part of Cirebon city in West Java and in the northern part of Semarang city in

Central Java, Indonesia. They were collected from boreholes during separated geotechnical investigation programs. The boreholes were drilled using a continuous coring method wherein the soil is continuously collected using a single core barrel with outer diameter of 76 mm and equipped with tungsten bit to cut the soil. Thin steel Shelby tubes with 73 mm OD, 70 mm ID, 67.5 mm opening diameter, 1.63 mm thick, and 760 mm in length were used to collect the undisturbed samples. The Shelby tubes were lowered to the bottom of hole and pushed hydraulically by the drilling rig. After recovery, the soil in the tube was protected from the elements by first scraping away some of the exposed soil from both ends of the tube and then coated with liquid paraffin. The tubes were transported by land to a soil mechanics laboratory in Bandung, West Java, Indonesia.

Standard Penetration Tests (SPT) were also performed using automatic trip hammer at every depth interval of 1.5 to 2 meter. The transferred energy of the SPT hammers vary between approximately 65 to 70 percent of the energy of free falling hammer. The SPT values measured near the sampling depths are given in Table 1. The zero SPT values mean that the SPT sampler penetrated the soil by its own weight. The SPT values shown as a range, i.e., the SPT's of S1, S2, S3, S5 samples, are SPT performed above and below the sample depths. The corrected SPT N_{60}values were determined based on an assumed hammer energy efficiency of 65 percent. Cone Penetration Tests with pore water measurement (CPTu) were also conducted near the boreholes location. The corrected cone resistance, q_t, profiles are shown in Figure 1. Also plotted on the figure are the location of the five collected samples.

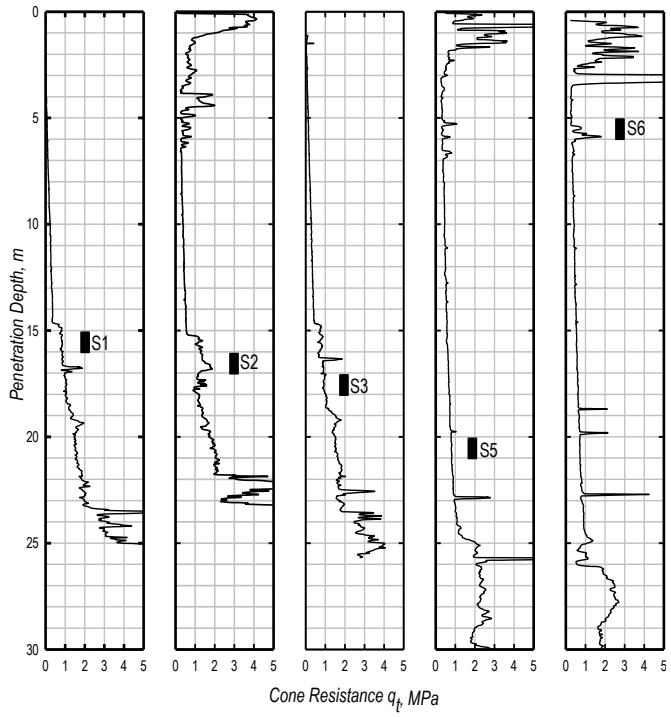

Figure 1 Corrected cone resistance profiles near the sampling boreholes

2.2 Test Specimens Preparation and Characteristics

All soil samples were pushed out from the Shelby tubes by a hydraulic extruder. The tubes were positioned horizontally during the extraction of the sample. About 100 mm long soil cores were pushed out from the tube and cut by a wire saw. The cores were placed standing up in a sampler holder and trimmed into test specimens with a diameter of 50 mm and a height of 100 mm. Some leftover soils from inside the tube and those resulted from trimming were used for determining the fines content passing the No. 200 sieve (ASTM D422), particle distribution of the fines content by hydrometer test (ASTM D7928), water content (ASTM D2216), and Atterberg Limits (ASTM D4318). Some samples from the same tubes have been subjected to companion unconfined compressive and consolidation tests.

The summary of all five samples characteristics is listed in Table 1. All samples have high fines content, i.e., particles passing the No. 200 sieve, in the range of about 89 to 97 percent. The Plasticity Index (*PI*) of these samples ranged from as low as 20 to as high as 91. Four of the samples are classified according to USCS as high plasticity fat clays (CH) and one, i.e., sample S6, as high plasticity elastic silt (MH). Sample S6 was collected from a thin layer of silt and has about 11 percent of fine sand. The presence of relatively high sand content in sample S6, in addition to shell fragments visually identified in the core retrieved by drilling, is indicated by relatively higher cone end resistances than those of the upper and lower layers and by cone resistance spikes along the depth interval from which the sample is collected (see Figure 1). The *PI* and *LL* of the five samples are plotted in plasticity chart shown in Figure 2 together with those of many samples collected from other boreholes performed in the same Semarang and Cirebon alluvial deposits. All samples have % clay content (< 0.002 mm) of more than 15 percent. According to Bol et al. (2010) and Pathak and Purandare (2016) they are not susceptible to liquefaction.

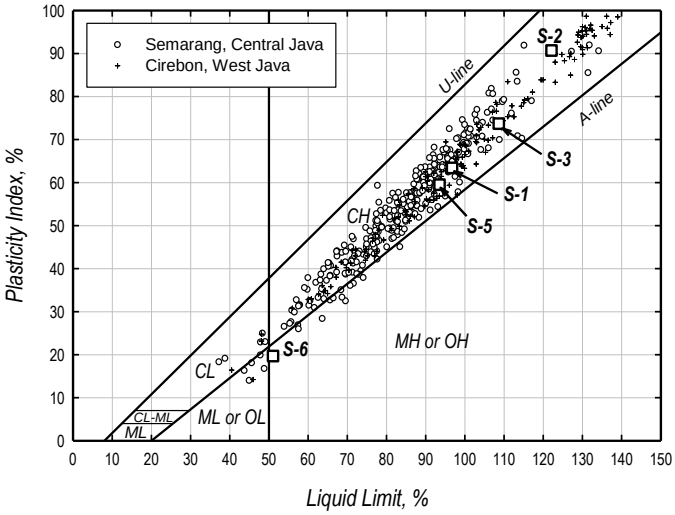

Figure 2 Plasticity Chart of alluvium clays and silts of Semarang and Cirebon North Java coastal deposit

Four of the samples, i.e., S2, S3, S5, and S6, were subjected to one-dimensional incremental loading consolidation test (ASTM D2435). Their e-log σ_v' consolidation curves are presented in Figure 3. The estimated preconsolidation pressure of each sample is given in Table 1. Not enough sample was available to carry out consolidation test on sample S1 thus its preconsolidation pressure could not be determined directly. The SPT N_{60} of sample S1 is around 4.3 blows/30 cm with average corrected cone end resistance q_t of around 980 kPa. Based on these SPT and cone end resistance values the undrained shear strength of sample S1 is estimated 40 kPa. In section 3.1 we explain that a normalized undrained shear strength, s_u/σ_c', of 0.46 is obtained from a normally consolidated clay whose characteristics are similar to our test specimens. Assuming that our specimens would have similar s_u/σ_c' of 0.46 then the *OCR* of sample S1 is estimated around 1.5. Sample S1 is located at a depth of 15 to 16 meter below the ground surface with calculated effective overburden pressure of 62.3 kPa. The preconsolidation pressure of sample S1 is thus estimated around 93.5 kPa.

The initial and after-consolidated w_c/LL and void ratios, initial preconsolidation stresses P_c' of our samples, and the final all around consolidation stresses σ_c' used in this study are given in Table 2. The final all around consolidation stresses σ_c' are the effective confining stresses applied to isotropically consolidate the samples passing their initial preconsolidation stresses to achieve an *OCR* of about 1.

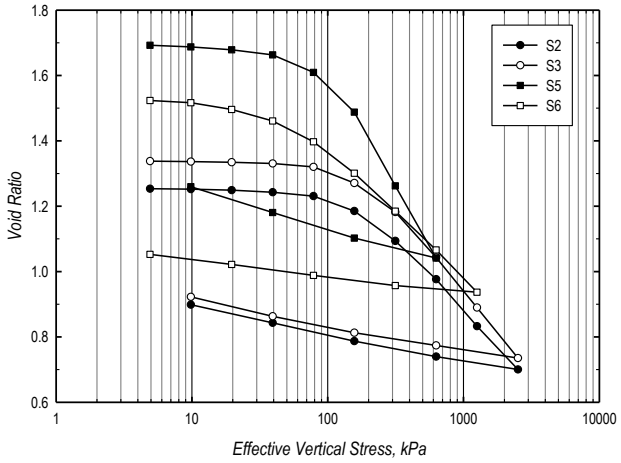

Figure 3 Consolidation e-log σ_v' curves of samples S2, S3, S5, and S6

Table 2 Initial and After Isotropically Consolidated Sample Characteristics

Sample No.	e_o		w_c/LL		P_c' (kPa)	Final σ_c' (kPa)
	Initial	Final*	Initial	Final*		
S1	1.34	1.03	0.58	1.29	93.5	104.9
S2	1.25	0.95	0.47	0.91	97.1	115.5
S3	1.34	0.35	0.51	1.05	197.1	223.8
S5	1.70	1.46	0.68	1.20	97.1	110.9
S6	1.53	1.27	1.45	2.14	87.3	125.2

Note: *After isotropically consolidated passing the initial preconsolidation stress

Figure 4 shows the plot of *PI* against the initial and after-saturated and consolidated w_c/LL ratio in the susceptibility-against-liquefaction-criteria chart of Bray and Sancio (2006). It can be seen that, based on soil activity, all samples in their in-situ conditions can be deemed non-susceptible to liquefaction but after the saturation and consolidation processes all samples have increased their water contents and w_c/LL ratios, supposedly increasing their sensitivity.

It is also of our interest to determine the quality of the soil samples used in this study. In order to do that, we followed the recommendation by Lunne et al. (2006), who suggested that the ratio between the change in void ratio Δe (the difference between the initial void ratio e_o and void ratio under in-situ effective overburden pressure e_i) and initial void ratio e_o is a good indicator of sample quality level. Lunne et al. (2006) criteria for evaluation of sample disturbance is given in Table 3.

Table 3 Sample quality criteria (Lunne et al., 2006)

OCR = 1 – 2	OCR = 2 – 4	Sample Quality Rating
$\Delta e/e_o$		
< 0.04	< 0.03	Very good to excellent
0.04 – 0.07	0.03 – 0.05	Good to fair
0.07 – 0.14	0.05 – 0.10	Poor
> 0.14	> 0.10	Very poor

Four of our samples have been subjected to consolidation test and their measured initial void ratios e_o and void ratios at their in-situ effective overburden pressure e_i, estimated from the *e-log* σ_v' consolidation curves, are given in Table 4 together with their $\Delta e/e_o$ ratios and sample quality rating. It can be seen that based on Lunne et al. (2006) sample quality criteria two samples were of very good to excellent quality, one sample was of good to fair quality, and one was of poor quality. Regardless of their initial quality rating, for our proposed study, all samples were isotropically consolidated (recompressed) passing their initial preconsolidation stress which to some extent would reduce sample disturbance and further increase the sample quality.

Table 4 Sample quality rating

Sample No	OCR	e_o	e_i	$\Delta e/e_o$	Quality Rating
S2	1.7	1.25	1.23	0.02	Very good to excellent
S3	1.8	1.34	1.30	0.03	Very good to excellent
S5	0.6	1.70	1.50	0.12	Poor
S6	1.4	1.53	1.43	0.07	Good to fair

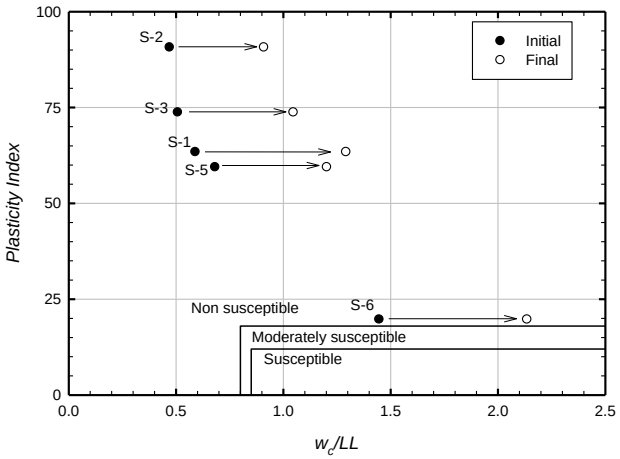

Figure 4 Initial and after consolidated samples w_c/LL plotted on susceptibility against liquefaction criteria chart (Bray and Sancio, 2006)

2.3 Test Procedures

2.3.1 Sample Preparation

The cyclic triaxial test is performed using a GDS Instrument device which has a compressive and tensile load capacity of +/- 5 kN with a cyclic load frequency up to 5 Hz and equipped with a 1.3-MPa capacity pneumatic pump for cell pressure and a 1-MPa back pressure pump. The pore water pressure is measured by a 1-MPa pressure transducer. The test specimens were wrapped with filter-paper side drains which have been cut to have 15 mm wide openings around the sample and enclosed with a 0.2 mm thick rubber membrane. A rubber suction cap is installed at the top cap to fix the submersible load cell to the top cap to ensure continuous contact during the cyclic loading. The triaxial cell is filled with water and about 10 mm of the top chamber is left empty to allow the water inside the cell to fluctuate during the upward and downward movement of the loading ram.

2.3.2 Saturation Process

The test sample is saturated by applying an initial 25 kPa back pressure and a 35 kPa cell pressure (ASTM D5311/D5311M-13). The volume of water entering the test sample is plotted against time to see the rate of water inflow. The sample degree of saturation is checked by evaluating the B-value. If the B-Value is less than 0.90 the saturation process is continued by increasing the backpressure while keeping 10 kPa difference to the cell pressure. The final applied back-pressures ranged from about 130 to 195 kPa. The final B-values varied from 0.90 to 0.99 indicative of "full" saturation.

2.3.3 Consolidation Process

Each specimen is consolidated isotropically to a target effective consolidation stress which is initially planned to be one and a half times its original preconsolidation stress. The all-around confining stress were applied in steps and the specimen is allowed to consolidate fully before the stress was increased. The consolidation process appeared to take a considerable time and because of the time constraint we decided to consolidate the samples to effective stress lower than the initial target effective stress (see Table 2). The pore pressure measure at the bottom sample is made sure to have dissipated and reached a constant value before the consolidation process is

ended. We observed that although the pore pressures have reached a fairly constant value, indicating the end of consolidation process, the measured pore pressures at the bottom end of each specimen u_c are found about 8 or 20 percent higher than the applied back pressures u_b. The average pore water pressure $\bar{u}$ inside the specimen was then calculated using Eq. (6) (Head and Epps 2014) and the final effective consolidation stress is calculated using Eq. (7). The final effective consolidation stresses σ_c' ranged from about 1.12 to 1.43 times the original preconsolidation stresses. We found that sample S-3 showed an uncharacteristic consolidation behavior, sudden and unusual large volume of water flowed out was recorded, and we therefore excluded this sample for further analysis.

$$\bar{u} = \frac{2}{3}u_c + \frac{1}{3}u_b \tag{6}$$

$$\sigma_c' = \sigma_c - \bar{u} \tag{7}$$

where,

$\bar{u}$ = average pore water pressure
u_c = pore water pressure at the bottom end of specimen
u_b = back pressure
σ_c = isotropic consolidation pressure

2.3.4 Cyclic Loading

After the consolidation process has been completed a load-controlled multistage cyclic axial load is applied to each test specimen. Each stage consists of 15 or 30 cyclic loads given in a sinusoidal form of uniform deviatoric axial cyclic stresses q_{cyc} with a frequency of 1 Hz which is a frequency commonly assumed for an earthquake loading (ASTM D5311/D5311M-13; Boulanger and Idriss 2004). Four specimens, i.e., S1, S2, S3, and S6, were subjected to fifteen-cycle load per stage and one specimen, i.e., S5, was subjected to thirty-cycle load per stage. The load-controlled cyclic load test is performed in undrained condition. Because of the limited number of samples and allocated time available for this study each specimen is subjected to a multistage load in which after a number of cyclic load has been applied a subsequent cyclic load is followed with the same number of cycles but with increased load amplitude and so on until failure is reached. Failure is defined as the condition where the mobilized cyclic resistance ceased to increase or started to decrease and/or a 5% double-amplitude axial strain is observed. During the cyclic load only the axial strains $\boldsymbol{\varepsilon_{cyc}}$ are recorded and converted to shear strains γ_{cyc} using Eq. (8) as suggested by Vucetic and Dobry (1991).

$$\gamma_{cyc} = 1.5 \times \varepsilon_{cyc} \tag{8}$$

The first deviator axial cyclic load q_{cyc} applied to each test specimen is +/- 0.01 kN which is equivalent to deviator stress of about +/- 5 kPa. In our study, the subsequent loads were applied almost immediately after the application of the previous load without letting the pore pressure induced by the previous loads to return to its initial level.

One of the records of the multistage load application and the accumulated induced pore pressure ratio against the load stage number is shown in Figure 5. This figure shows a total of nineteen load stages each consists of 15 cyclic loads. As explained earlier, the subsequent load was applied immediately without letting the induced pore pressure from the previous load to dissipate. It can be seen that the induced pore pressure appears to be small, especially during the early load stages, and rise to only about 20 percent of the effective consolidation stress, when the sample reached its maximum cyclic strength.

Figure 6 shows the records of one of the stages in which a cyclic deviatoric stress q_{cyc} of 75 kPa was applied. It can be seen here that, especially at high deviatoric stress levels, the first load cycle sometimes overshot the load target before it finally stabilized (Figure 6(a). Other records include the induced pore water pressures, presented as pore pressure ratio, r_u, (Figure 6(b), 6(c), 6(d)) and axial strains (Figure 6(d)). It can be seen here that there is a lag between the application of the cyclic deviatoric stress and the response of the induced pore pressure (Figure 6(b)), thus creating a loop when the pore pressure is plotted against the deviatoric stress (Figure 6(c)). On the other hand, the induced pore pressure reacted in phase with the sample axial strains (Figure 6(d)).

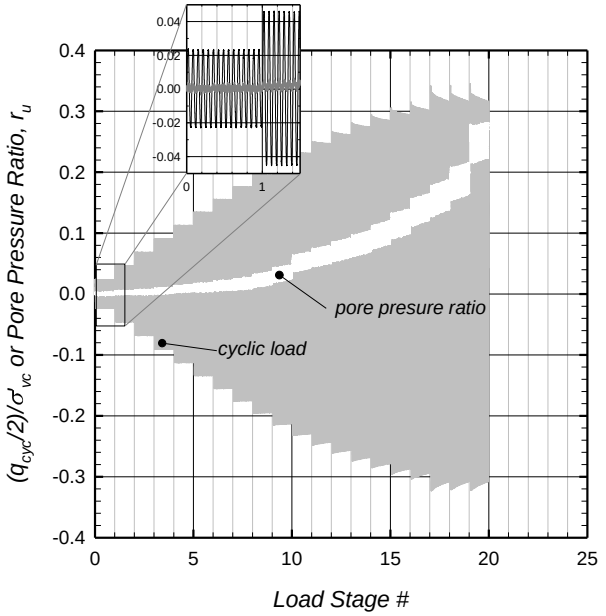

Figure 5 Multistage Cyclic Load and Accumulated Cyclic-Induced Pore Pressure

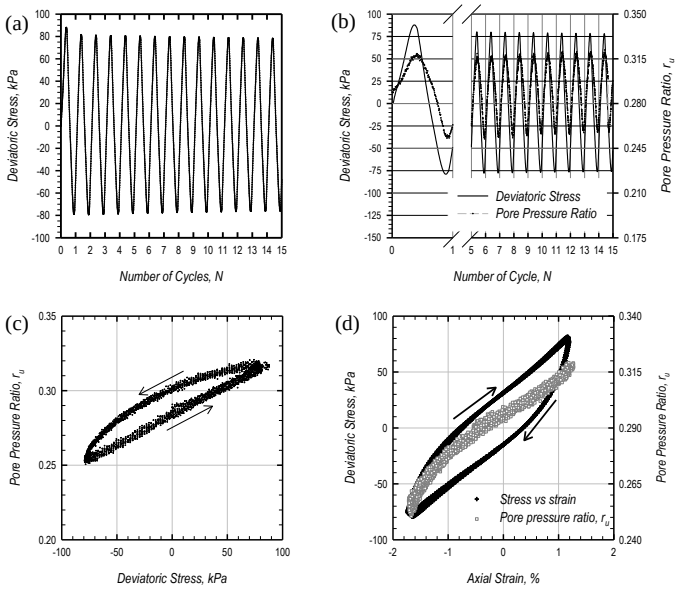

Figure 6 Records of cyclic load and pore pressure ratio versus number of cycles and the behavior of cyclic-induced pore pressure versus deviatoric stress and axial strain of sample S-6 at a deviatoric stress of 75 kPa

3. RESULTS AND DISCUSSIONS

3.1 Cyclic Strength Ratio

As explained earlier the number of test specimens is limited and all of them were used for the cyclic test. There was no more core samples from the same tubes available for determining their after-consolidated undrained shear strength. In order to estimate their after-consolidated undrained shear strength we assumed that they follow the normalized

undrained strength concept and that SHANSEP equation is applicable to our samples. We then used one sample from a different location but still from the north of Java to determine its s_u/σ_c' under normally-consolidated state (*OCR* = 1). This sample has about 90% fines content with *LL* of 93 and *PI* of 62. The sample wet density is around 16 kN/m^3 with a measured preconsolidation pressure of 143.2 kPa. It was collected from a depth of 2.5 meter and was further isotropically consolidated passed its initial preconsolidation pressure to an average effective pressure σ_c' of 170.9 kPa. The sample was subjected to a static undrained axial compressive load to a maximum and failed at a deviatoric stress of 157.6 kPa and thus an undrained shear strength of 78.8 kPa. The sample normalized undrained shear strength, s_u/σ_c', of approximately 0.46 at *OCR* of 1 is then obtained. Using this normalized undrained shear strength we determined our samples undrained shear strength estimates based on their final effective consolidation stresses. The estimated undrained shear strength of the samples after isotropically consolidated to their final consolidation stresses are given in Table 5.

Table 5 Samples estimated undrained shear strength after isotropically consolidated

Sample No	Final σ_c' (kPa)	Estimated s_u (kPa)
S1	104.9	48.3
S2	115.5	53.1
S3	223.8	102.9
S5	110.9	51.0
S6	125.2	57.6

Figure 7 shows the curves of cyclic strength ratio, $(q_{cyc}/2)/s_u$, versus shear strain from the multistage loading of sample S-6. The backbone curve connecting the points reached at the end of each stage is also shown. From this backbone curve the cyclic strength ratio of sample S-6 is approximately 0.71. The cyclic strength ratio of the other samples included in our analysis is around 0.72 for samples S-2 and S-5 and about 0.65 for sample S-1. The average cyclic strength ratio of these four samples is around 0.70. At this time we excluded sample S-3 from our analysis because we still cannot found the explanation of its suspect consolidation behavior.

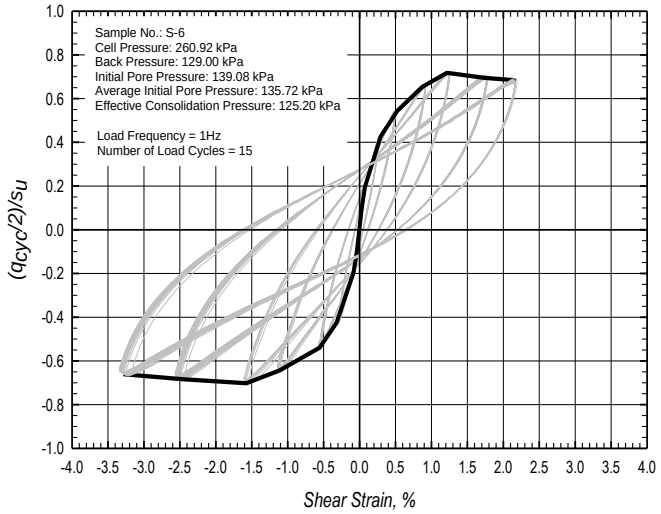

Figure 7 Sample S-6 cyclic strength ratio versus shear strain from multistage loading and the backbone curve

Cyclic strength ratios of our samples are plotted against PI in Figure 8. This figure shows that PI does not appear to have clear influence on the cyclic strength ratio of our samples. We also plotted in Figure 8 the results from other researchers as reported by Boulanger and Idris (2007). They used natural and tailing silts/clays which were subjected to either cyclic triaxial or direct simple shear (*DSS*) tests. The cyclic strength ratios indicated in Figure 8 vary from about 0.65 to 1. As explained earlier our samples undrained shear strengths were not measured but estimated based on the normalized undrained shear strength, s_u/σ_c', of 0.46 which was determined on a sample collected from a different site but with similar index properties.

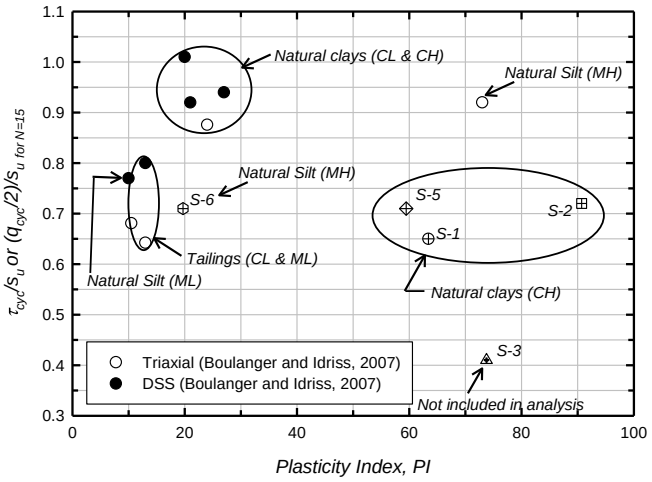

Figure 8 Cyclic Strength Ratio (N=15) versus Plasticity Index

3.2 Cyclic Resistance Ratio

The backbone curves of the cyclic resistance ratio (CRR) of our four samples are plotted against the shear strain from the multistage loads are in Figure 9. The *CRR* of our samples were determined as the mobilized maximum cyclic stress ratios. The normalized stress-strain curves have similar shape and fall within a very narrow range with an average *CRR* of about 0.31.

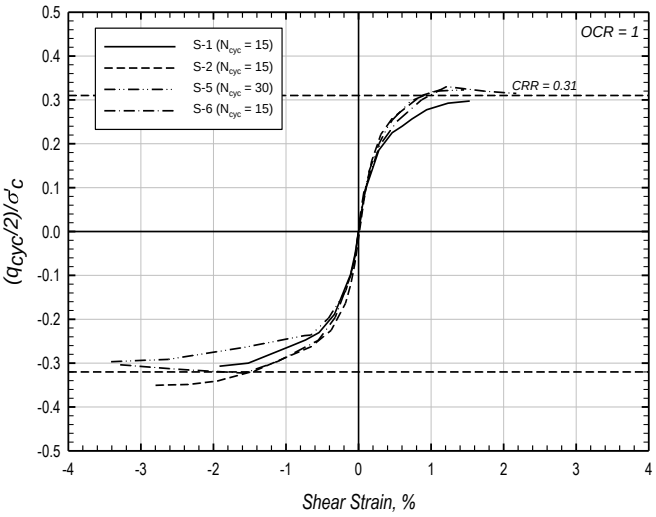

Figure 9 Backbone curve of Cyclic Resistance Ratio (CRR) versus shear strain of samples S-1, S-2, S-5, and S6

The *CRR* of the four samples are plotted against *PI* in Figure 10 together with other results reported by Boulanger and Idriss (2007) and Pekcan et al. (2004). Our four samples *CRR*s vary in a very narrow range between about 0.30 and 0.32. Boulanger and Idriss (2007) results of tailing clays and silts (CL, ML) and natural clays (CL, CH) with *PI* less than 30 are consistently lower than our findings and fall within a narrow range of about 0.2 to 0.25 but one result of natural silt (MH), whose PI is about 72 and tested using a cyclic triaxial, has a *CRR* of about 0.35 which is close to our findings.

Pekcan et al. (2004) results shown in Figure 10 are from their study on cyclic resistance of eleven clayey silt and silty clay samples from Adapazari, Turkey. Four of their findings, i.e., those with medium *PIs*, were used here for comparison. As can be seen in Figure 10, the four samples, reported as natural clays (CH), yielded *CRR*

values in the range between about 0.55 and 0.80 which are consistently much higher than both our findings and those of Boulanger and Idriss (2007). A reasonable explanation of why they are much higher is as follows. The samples used by Pekcan et al. (2004) were collected from a depth of about 3.5 and 4.5 m with ground water level depths reported at about 0.4 to 1.4 m below the ground surface. We estimated that the existing effective overburden stress at the sample depths is about 25 and 35 kPa and Pekcan et al. (2004) isotropically consolidated these samples to 50 kPa before the cyclic loads were applied. There is no information regarding the *OCR* values of the samples presented by Pekcan et al. (2004), but considering the possible ground water level fluctuation and desiccation effects commonly experienced by the soil near the surface, there is a possibility that their samples were in overconsolidated state and that the 50 kPa consolidation stress was not high enough to bring the samples to a normally consolidated state. Overconsolidated clays are expected to have higher *CRR* than those of normally consolidated clays.

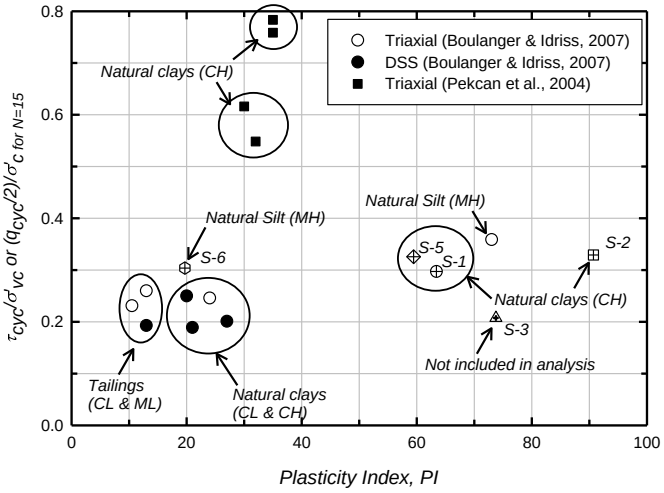

Figure 10 Cyclic Resistance Ratio (N=15) versus Plasticity Index

4. CONCLUSIONS AND RECOMENDATIONS

At a normally consolidated state with *OCR* of about 1 the magnitude of cyclic strength ratio and cyclic resistance ratio (*CRR*) of our clay-like behavior fine-grained soils from North Java coastal plains fall within a very narrow range with an average cyclic strength ratio, $(q_{cyc}/2)/s_u$, of around 0.70 and an average *CRR*, $(q_{cyc}/2)/\sigma_c'$, of about 0.31. In other words, the cyclic strength of normally consolidated clays and silt is about 70 percent of their undrained shear strength and about 31 percent of their effective consolidation pressure. Our laboratory test results suggested that the cyclic shear strength of our samples have a very strong relationship with both undrained shear strength and effective consolidation pressure.

The normalized cyclic stress-strain behavior of our samples appear to follow the SHANSEP concept, although further study is required to proof that the *CRR* of clay-like behavior fine-grained soils do have a unique relationship with *OCR*.

This study also supports the findings of other researchers that *PI* does not influence the magnitude of cyclic strength ratio and cyclic resistance ratio (*CRR*) of clay-like behavior fine-grained soils.

5. ACKNOWLEDGEMENTS

The authors are grateful to the P3MI Program of Institute of Technology Bandung and Soilens Soil Mechanics Laboratory for supporting this research.

6. REFERENCES

Bol, E., Önalp, A., Arel, E., Sert, S., and Özocak, A. (2010) "Liquefaction of silts: the Adapazari criteria", *Bulletin of Earthquake Engineering*, *8*(4), pp859-873

Boulanger, R. W., and Idriss, I. M. (2004) "Evaluating the Potential for Liquefaction or Cyclic Failure of Silts and Clays", Report No. UCD/CGM-04/01, Center for Geotechnical Modeling, University of California at Davis.

Boulanger, R. W., and Idriss, I. M. (2006) "Liquefaction Susceptibility Criteria for Silts and Clays". Journal of Geotechnical and Geoenvironmental Engineering, ASCE 132:11, pp1413-1424.

Boulanger, R. W., and Idriss, I. M. (2007) "Evaluation of Cyclic Softening in Silts and Clays", Journal of Geotechnical and Geoenvironmental Engineering, ASCE 133:6, pp641-652.

Bray, J. D., and Sancio, R. B (2006) "Assessment of the Liquefaction Susceptibility of Fine-Grained Soils", Journal of Geotechnical and Geoenvironmental Engineering, ASCE 132:9, pp1165-1177.

Head, K. H., and R. J. Epps. (2014) "Manual of Soil Laboratory Testing", Volume 3: Effective Stress Test, Whittles Publishing, Scotland.

Ladd, C. C., and Foott, R. (1974) "New Design Procedure for Stability of Soft Clays", Journal of the Geotechnical Engineering Division, ASCE 100:7, pp763-785.

Lunne, T., Berre, T., Andersen, K. H., Strandvik, S., and Sjursen, M. (2006) "Effects of Sample Disturbance and Consolidation Procedure on Measured Shear Strength of Soft Marine Norwegian Clays", Canadian Geotechnical Journal, 43, pp726-750.

Pathak, S. R. and Purandare, A. S. (2016) "Liquefaction Susceptibility Criterion of Fine Grained Soil", International Journal of Geotechnical Engineering 10(5), pp445-459

Pekcan, O., Cetin, K. O., and Bakir, B. S., (2004) "Cyclic Behavior of Adapazari Silt and Clay Mixtures", Proceedings of 11th ICSDEE/3rd ICEGE, pp676-681.

Seed, H. B., and Idriss, I. M. (1982) "Ground Motions and Soil Liquefaction During Earthquakes", Berkeley, California, EERI Monograph.

Seed, H. B., Idriss, I. M., and Arango, I. (1983) "Evaluation of Liquefaction Potential Using Field Performance Data", Journal of Geotechnical Engineering, ASCE 109:3, pp458-482.

Vucetic, M., and Dobry, R. (1991) "Effect of Soil Plasticity on Cyclic Response", Journal of Geotechnical Engineering, ASCE 117:1, pp89-107.

Wang, W. (1981) Some Findings in Soil Liquefaction, Report Water Conservancy and Hydro-electric Power Scientific Research Institute, Beijing, China. pp1-17.